



ISSN 1110-0451



(E S N S A)

## Potentiometric Sensing of Thorium Ions Using PVC Matrix Electrodes Based on Crown Ethers

**Zeinab F. Akl**

*Nuclear Safeguards and Physical Protection Department, Egyptian Atomic Energy Authority (EAEA), P.O. Box 7551, Cairo, Egypt.*

### ARTICLE INFO

*Article history:*

Received: 28<sup>th</sup> Jan. 2023

Accepted: 1<sup>st</sup> Mar. 2023

Available online: 7<sup>th</sup> June 2023

*Keywords:*

Thorium determination;

Potentiometric sensors;

PVC membranes;

Water analysis;

18-Crown-6-ether derivatives.

### ABSTRACT

New potentiometric membrane sensors have been designed to measure  $\text{Th}^{4+}$  ions using two derivatives of 18-crown-6-ether as neutral ion-carriers. The membrane composition was optimized through a multi-stage process regarding plasticizers, lipophilic ionic additives, and ion-carrier content and the corresponding sensors' performance characteristics were investigated. The optimized sensors exhibited a Nernstian behavior for  $\text{Th}^{4+}$  ions over wide working concentration and pH ranges. The sensors' repeatability, reproducibility, and reversibility were tested under the optimal conditions. The selectivity studies indicated the selective behavior of the developed sensors towards  $\text{Th}^{4+}$  ions with respect to various mono, di, and trivalent ions. The sensors possess a fast response time and can work for at least 12 weeks without significant changes in their sensitivity.  $\text{Th}^{4+}$  ions concentration in water samples was directly assessed by the developed sensors with good recovery and relative standard deviation values indicating the accuracy and precision of the developed sensors. Moreover, the obtained results were in a good agreement with those obtained by the spectrometric method.

## 1. INTRODUCTION

In view of the climate change threat, nuclear energy has gained increased interest among various States as a clean and low-carbon energy system with low operating cost [1]. Although the vast majority of current nuclear reactors are based on uranium, thorium is regarded as a potential fuel in the nuclear energy industry. Thorium is a fissionable material which is more naturally abundant than uranium and thus can be introduced as an energy source to some types of nuclear reactors [2-3]. The large-scale industrial and technological applications of thorium shared in its distribution over the earth's surface through mining, processing, usage, and waste disposal [4]. Thorium is ubiquitously distributed in soil, rocks, sand, plants, and water; thus it may end up in the human food chain causing acute health effects. Thorium's non-biodegradability nature and ability to accumulate in human tissues can cause irreversible health consequences and harmful diseases [5].

Thorium's long-time persistence in soils and ecological systems and its well-known environmental hazards have

stimulated the development of sensitive and reliable analytical tools for thorium quantification [6]. Thus, various analytical techniques, based on thorium's chemical, physical, or radiation characteristics have been adopted to support routine control measurements, radiological impact assessment of various anthropogenic activities, and radiation protection [7-11]. However, those techniques demand expensive instruments, prior treatment, or high running costs. On the other hand, electrochemical detection of thorium [12] is a powerful tool that can overcome those shortcomings with its promising features such as cost-effectiveness, user-friendly, good precision, accuracy, quick response, and portability. Electrochemical sensors can measure various analytes directly without earlier separation processes, leading to a simpler determination procedure compared to other analytical methods. There have been some reports on the potentiometric sensing of thorium ions using ion-selective electrodes (ISEs) based on various ion-carriers [12-18]. However, new electrode architectures with increased sensitivity and enhanced selectivity are demanded.

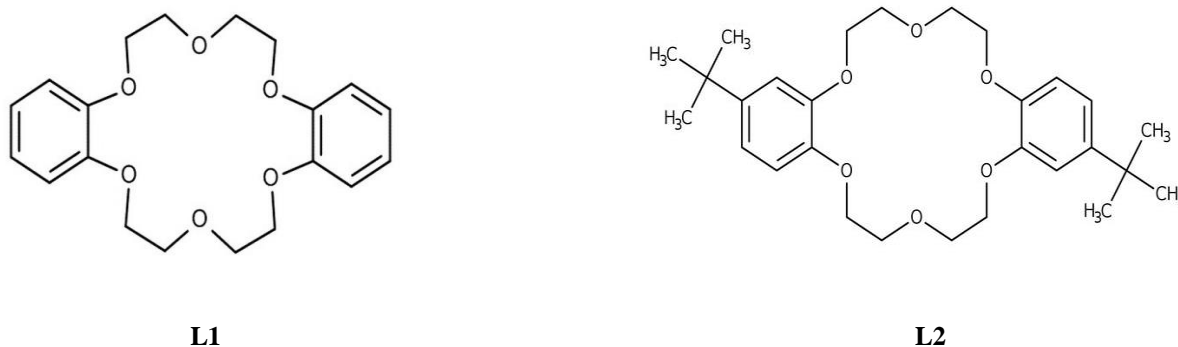


**Fig. (1): Chemical structure of the ionophores: dibenzo-18-crown-6 (L1) and di-tert-butyl-dibenzo-18-crown-6 (L2).**

Crown ethers are among the sensing materials that were reported as suitable neutral carriers for ISEs construction [19]. They are hetero-cyclic chemical compounds having rings with multiple ether linkages; which can form stable complexes with various metal ions thanks to their cavity-cation fit. Crown ethers have a hydrophobic ring surrounding a hydrophilic cavity and are stabilized by the lone electron pairs of the oxygen atoms; therefore, they have outstanding cations complexing ability via the ring's cavity [20]. The selectivity of crown ethers toward a certain ion is dependent on the ring's size as well as the nature of hetero-substituent on the ring. Owing to their unique structure, ease of structural modification, and selective molecular recognition; crown ethers have been employed in separation and determination of various metal ions [21-23]. Although crown ethers with various cavity sizes and substituents have been extensively studied as selective carriers in several cation-selective sensors, no reports are available to the author's knowledge on their application for  $\text{Th}^{4+}$  ISEs; In view of these aspects,  $\text{Th}^{4+}$  PVC membrane-ISEs based on dibenzo-18-crown-6 (L1) and di-tert-butyl-dibenzo-18-crown-6 (L2) (Fig. 1) are described in the present study. The potentiometric properties of the developed sensors were evaluated which revealed that the sensors have a wide working ranges with good detection limits.

## 2. EXPERIMENTAL

### 2.1. Reagents

Dibenzo-18-crown-6, di-tert-butyl-dibenzo-18-crown-6, polyvinyl chloride (PVC), dioctyl phthalate (DOP), o-nitrophenyl octyl ether (o-NPOE), dioctyl sebacate (DOS), 1-chloronaphthalene (CN), tris(2-ethylhexyl) phosphate (TEHP), potassium tetrakis(4-chlorophenyl) borate (KTPCIPB), tridodecylmethylammonium chloride

(TDMACl), and tetrahydrofuran (THF) were obtained from Merck or Sigma-Aldrich. Arsenazo III (3,6-bis[(2-arsenophenyl)-azo]-4,5-dihydroxy-2,7-naphthalene-disulfonic acid) was received from Fluka.

### 2.2. Construction of the sensors

The general procedure to prepare the working membranes was dissolving the required amount of PVC, plasticizer, lipophilic salt, and crown ether of total weight of 0.2 g in THF (2.0 mL). After vigorous shaking, the mixture was transferred to a glass ring (22 mm internal width) put above an appropriate glass slide. When the THF was completely evaporated, the membrane was cut into circles of adequate size and bonded to a PVC tube using PVC slurry. Then, the sensors were filled with the interior reference solution, conditioned overnight in  $10^{-3}$  mol  $\text{L}^{-1}$   $\text{Th}^{4+}$  ions solution, and washed thoroughly before use by deionized water.

### 2.3. Potentiometric measurements

An ion analyzer data acquisition system (Nico2000 Ltd., UK) was used for potentials recording at  $25.0 \pm 0.1$  °C. The conditioned sensors were immersed along with silver-silver chloride reference electrode (Sentek, UK) into the sample solution and were allowed to equilibrate till a steady potential values were obtained. The potentiometric response characteristics of the sensors were examined through measuring the cell potentials in response to the successive variation of  $\text{Th}^{4+}$  ions concentrations and plotting a calibration graph for  $-\log [\text{Th}^{4+}]$  versus the cell potentials. The cell assembly could be represented as: Ag/AgCl | filling solution | PVC membrane | test solution | reference electrode (Silver-silver chloride).

The impact of the solution's pH on the sensors' potential readings was observed over a pH range from

2.0 to 9.0 at two fixed  $\text{Th}^{4+}$  ions concentrations ( $10^{-4}$  and  $10^{-3}$  mol  $\text{L}^{-1}$ ) by adding  $\text{HNO}_3$  or  $\text{NaOH}$ . pH monitoring was made through a digital pH meter (Jenway, UK).

To evaluate the dynamic response time, the optimized sensors were immersed successively into various  $\text{Th}^{4+}$  ions solutions each with a ten-fold concentration difference. The response time was determined as the average time taken by the sensor to attain stable and low noise potential with a value of  $\pm 1$  mV of the equilibrium value.

The impact of the interfering ions on the sensors' response was experimentally investigated and described in terms of the selectivity coefficients,  $\log (K_{\text{Th},j}^{\text{pot}})$  by the modified separate solution method [24]. According to this method, readings (mV) were measured for a series of interfering ions (j) and primary ion ( $\text{Th}^{4+}$ ) then the selectivity coefficients were calculated using the following equation [25]:

$$K_{\text{Th},j}^{\text{pot}} = \exp \left( \frac{z_{\text{Th}} F (E_j^0 - E_{\text{Th}}^0)}{RT} \right)$$

where R is the gas constant, T is the absolute temperature, F is the Faraday constant,  $E_{\text{Th}}^0$  and  $E_j^0$  are the potentials measured at 1 M for Th and interfering ions, and  $z_{\text{Th}}$  is the charge of the Th ion.

#### 2.4. Determination of $\text{Th}^{4+}$ ions content in aqueous samples

Various water samples were collected, filtered, transferred to a 50-mL beaker, and then the pH was adjusted to 4. The samples were spiked with known aliquots of  $\text{Th}^{4+}$  ions solution at three different levels, then the sensor set containing the optimized sensors in conjunction with the reference electrode was immersed into the sample solution and the corresponding potential readings were recorded. Prior to the measurement process, calibration was carried out and the corresponding linear equation was obtained. The obtained potential values were referred to this calibration curve to calculate  $\text{Th}^{4+}$  ions content.

$\text{Th}^{4+}$  ions concentration in the same samples was also determined by the reference spectrophotometric method using a double beam UV-Visible spectrophotometer (Thermo Evolution 300- England). This method is based on the formation of colored complexes of  $\text{Th}^{4+}$  ions and Arsenazo III that could be measured at  $\lambda_{\text{max}}$  of 654 nm [26].

### 3. RESULTS AND DISCUSSION

#### 3.1. Potentiometric characterization of the developed sensors

To attain the best potentiometric performance of the sensors, the optimum membrane composition was initially determined. Literature shows that the response characteristics of polymeric membrane ISEs depend on the membrane ingredients [27]; accordingly, various aspects of membranes containing (L1) and (L2) were investigated. Table 1 summarizes the corresponding potentiometric characteristics.

Membranes incorporating the same amount of different plasticizers viz DOS, CN, DOP, NPOE, and TEHP were fabricated; while keeping the content of the ion-carrier, PVC, and KTpCIPB constant in order to investigate the plasticizer's impact on the electrode response characteristics. Previous reports show that polymeric membranes with plasticizer proportion double that of the PVC are characterized by optimal physical properties and fairly high mobility of the ingredients [28], therefore the same ratio was used throughout the current work. Examination of Table 1 shows that the sensors plasticized with TEHP have better response characteristics for both crown ethers, viz. better slope, wider working range, and lower detection limit. This indicates the high mixing ability of TEHP and PVC that results in the production of a homogeneous membrane with proper mechanical properties. Additionally, it can be concluded that TEHP provides an adequate diffusional mobility of the crown ethers in the membrane and a good complexation environment between the crown ethers and  $\text{Th}^{4+}$  ions [29].

To understand how the ion-carrier's amount could impact the sensors' response characteristics, various mass percentages of the crown ethers were used; and the results showed that 3% crown ether (w/w) was the optimum ion-carrier ratio. Lower ion-carrier percentages led to poor calibration slope while the higher ones result in unstable response performance of the sensors due to saturation of the membrane and irregular ion-carrier distribution in the membrane [30]. Considerable improvement in the sensors' performance was observed by adding negatively charged lipophilic additives to the membrane composition. It is clear from Table 1 that better response characteristics in terms of slope, detection limit, and linear range are noticed by increasing the KTpCIPB proportion in the membrane. Such improvement in the response behavior resulted from the ability of KTpCIPB to increase the membrane's electrical conductivity, reduce the membrane's ohmic resistance, and enhance the exchange kinetics at the sample-membrane leading to better sensitivity [31]. It can be seen that 1.5% of KTpCIPB is the suitable lipophilic additive ratio and higher proportions results in lower calibration slopes.

The working mechanism of the ion-carrier was evaluated from the charge effect of the lipophilic ionic additives on the sensor's response. To this end, membranes containing cationic or anionic lipophilic additives at the same percentage were prepared and their potentiometric response was investigated and represented in Table 1. An anionic response was produced when lipophilic cationic sites (TDMACl) were added to the membrane; while an improved response towards  $\text{Th}^{4+}$  ions was observed by adding anionic additives (KTpCIPB). Generally, cation-selective sensors with neutral carriers require lipophilic anionic additives to obtain a Nernstian response, while cationic additives are required in the case of charged carriers [32]. A perusal of Table 1 displays the enhanced response characteristics with anionic additives, suggesting that these crown ethers act as neutral carriers.

Electrodes 18 and 21 with composition of crown ether: TEHP: PVC: KTpCIPB in the ratio of 3: 63.5: 32: 1.5

w/w exhibit superior potentiometric behavior and were used for further potentiometric measurements. The calibration curve for the optimized sensors towards various  $\text{Th}^{4+}$  ion concentrations is illustrated in Fig. 2. These sensors displayed linearity to  $\text{Th}^{4+}$  ions in wide working concentration range of  $1.0 \times 10^{-6} - 1.0 \times 10^{-1}$  and  $1.0 \times 10^{-7} - 1.0 \times 10^{-1} \text{ mol L}^{-1}$  with calibration slopes of 14.41 and 14.85 mV decade<sup>-1</sup> and detection limits of  $5.27 \times 10^{-7}$  and  $6.65 \times 10^{-8} \text{ mol L}^{-1}$  for sensors 18 and 21, respectively.

It can be noted that the optimized sensor based on L2 reveals better potentiometric response characteristics than the sensor based on L1 indicating its better solubility in the membrane. Additionally, the electron-donating nature of the tertiary butyl groups lead to increasing the electron density of the oxygen atoms, resulting in a better extraction ability of L2 [33].

**Table (1): Membrane compositions and corresponding response characteristics of the developed sensors**

Sensor no.	Membrane Composition % (mass, w/w)					Analytical Parameters		
	L1	L2	PVC	Plasticizer	Additives	Slope, mV decade <sup>-1</sup>	Linear Range, mol L <sup>-1</sup>	Detection Limit, mol L <sup>-1</sup>
1	2.0	–	32.5	o-NPOE, 65.5	–	11.28	$5.0 \times 10^{-5} - 1.0 \times 10^{-2}$	$2.32 \times 10^{-5}$
2	2.0	–	32.5	DOP, 65.5	–	12.30	$5.0 \times 10^{-5} - 1.0 \times 10^{-1}$	$1.54 \times 10^{-5}$
3	2.0	–	32.5	TEHP, 65.5	–	13.28	$1.0 \times 10^{-5} - 1.0 \times 10^{-1}$	$8.05 \times 10^{-6}$
4	2.0	–	32.5	DOS, 65.5	–	11.05	$1.0 \times 10^{-5} - 1.0 \times 10^{-1}$	$2.21 \times 10^{-5}$
5	2.0	–	32.5	CN, 65.5	–	10.87	$1.0 \times 10^{-4} - 1.0 \times 10^{-1}$	$8.72 \times 10^{-5}$
6	–	2.0	32.5	o-NPOE, 65.5	–	12.82	$1.0 \times 10^{-5} - 1.0 \times 10^{-2}$	$7.10 \times 10^{-6}$
7	–	2.0	32.5	DOP, 65.5	–	13.62	$5.0 \times 10^{-6} - 1.0 \times 10^{-1}$	$1.52 \times 10^{-6}$
8	–	2.0	32.5	TEHP, 65.5	–	14.07	$1.0 \times 10^{-6} - 1.0 \times 10^{-1}$	$7.94 \times 10^{-7}$
9	–	2.0	32.5	DOS, 65.5	–	13.23	$5.0 \times 10^{-6} - 1.0 \times 10^{-1}$	$1.00 \times 10^{-6}$
10	–	2.0	32.5	CN, 65.5	–	11.27	$5.0 \times 10^{-5} - 1.0 \times 10^{-2}$	$5.82 \times 10^{-6}$
11	1.0	–	33.0	TEHP, 66.00	–	12.25	$1.0 \times 10^{-5} - 1.0 \times 10^{-1}$	$8.00 \times 10^{-6}$
12	3.0	–	32.5	TEHP, 64.50	–	13.95	$1.0 \times 10^{-6} - 1.0 \times 10^{-1}$	$8.24 \times 10^{-7}$
13	4.0	–	32.0	TEHP, 64.00	–	13.01	$5.0 \times 10^{-6} - 1.0 \times 10^{-1}$	$1.92 \times 10^{-6}$
14	–	1.0	33.0	TEHP, 66.00	–	12.84	$5.0 \times 10^{-6} - 1.0 \times 10^{-1}$	$1.00 \times 10^{-6}$
15	–	3.0	32.5	TEHP, 64.50	–	14.38	$1.0 \times 10^{-6} - 1.0 \times 10^{-1}$	$5.46 \times 10^{-7}$
16	–	4.0	32.0	TEHP, 64.00	–	14.17	$1.0 \times 10^{-6} - 1.0 \times 10^{-1}$	$5.00 \times 10^{-7}$
17	3.0	–	32.0	TEHP, 64.0	KTpCIPB, 1.0	14.24	$1.0 \times 10^{-6} - 1.0 \times 10^{-1}$	$6.82 \times 10^{-7}$
18	3.0	–	32.0	TEHP, 63.5	KTpCIPB, 1.5	14.41	$1.0 \times 10^{-6} - 1.0 \times 10^{-1}$	$5.27 \times 10^{-7}$
19	3.0	–	31.5	TEHP, 63.0	KTpCIPB, 2.5	14.13	$1.0 \times 10^{-6} - 1.0 \times 10^{-1}$	$4.53 \times 10^{-7}$
20	–	3.0	32.0	TEHP, 64.0	KTpCIPB, 1.0	14.87	$1.0 \times 10^{-6} - 1.0 \times 10^{-1}$	$1.48 \times 10^{-7}$
21	–	3.0	32.0	TEHP, 63.5	KTpCIPB, 1.5	14.85	$1.0 \times 10^{-7} - 1.0 \times 10^{-1}$	$6.65 \times 10^{-8}$
22	–	3.0	31.5	TEHP, 63.0	KTpCIPB, 2.5	14.51	$1.0 \times 10^{-7} - 1.0 \times 10^{-1}$	$7.54 \times 10^{-8}$
23	3.0	–	32.0	TEHP, 63.5	TDMACl, 1.5	-19.42	$1.0 \times 10^{-4} - 1.0 \times 10^{-1}$	$9.72 \times 10^{-5}$
24	3.0	–	31.5	TEHP, 63.0	TDMACl, 2.5	-21.42	$1.0 \times 10^{-4} - 1.0 \times 10^{-1}$	$9.54 \times 10^{-5}$
25	–	3.0	32.0	TEHP, 63.5	TDMACl, 1.5	-20.39	$1.0 \times 10^{-6} - 1.0 \times 10^{-1}$	$9.90 \times 10^{-7}$
26	–	3.0	31.5	TEHP, 63.0	TDMACl, 2.5	-23.43	$1.0 \times 10^{-6} - 1.0 \times 10^{-1}$	$9.78 \times 10^{-7}$

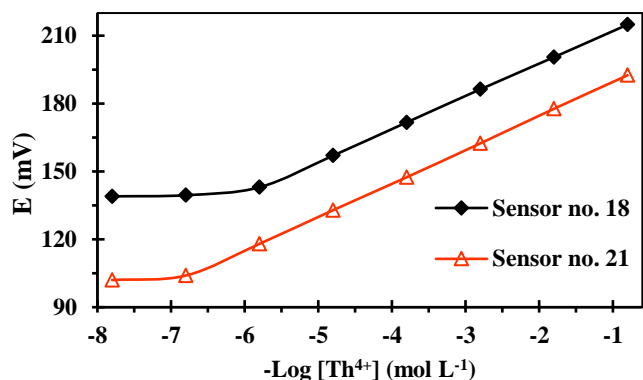


Fig. (2): Calibration graphs for sensor no. 18 (◆) and sensor no. 21 (Δ).

### 3.2. Dynamic response time, reversibility, and working life

The dynamic response of the developed sensors was tested according to the IUPAC recommendations [34] to determine the time needed to reach a limiting potential after immersing the sensors into  $\text{Th}^{4+}$  ions solutions. The potential versus time plot of the developed sensors is given in Fig. 3A. The dynamic response time was found to be 10 and 8 s for sensors no. 18 and no. 21, respectively. This short response time could result from the fast diffusion equilibrium of  $\text{Th}^{4+}$  ion achieved between the aqueous layer and the ISE membrane in addition to the fast exchange kinetics of complexation–decomplexation of  $\text{Th}^{4+}$  with the crown ethers at the solution–sensor interface [35].

To investigate the sensors' reversibility, potentials were measured in solutions with different concentrations of  $\text{Th}^{4+}$  ions ( $1.0 \times 10^{-7}$  –  $1.0 \times 10^{-1}$  mol L<sup>-1</sup>) first in ascending concentration order followed by a descending one. It is apparent from Fig. 3B that the sensors' response toward  $\text{Th}^{4+}$  ions solutions is reversible.

The lifetime of the optimized sensors were tested to assess their ability to maintain their performance for a certain period of time. The sensors' potentiometric responses were periodically recorded by measuring the potentials at standard  $\text{Th}^{4+}$  ions solutions ( $1.0 \times 10^{-7}$  to  $1.0 \times 10^{-1}$  mol L<sup>-1</sup>) in 16 weeks duration. By investigating the calibration curve slope as depicted in Table 2, it can be concluded that the sensors can be utilized for at least 12 weeks with no discernible difference in their behavior. After this period the calibration slope drifted away from the Nernstian behavior and a change in the working range was observed. This could result from the leak of the membrane constituents into the solution.

### 3.3. pH sensitivity

To assess the sensors' pH usable range, the potentiometric response measurements were carried out in pH range from 2.0 to 9.0. The sensors' potential change with the pH of the solution is shown in Fig. 4. It was observed that sensors based on L1 and L2 behave similarly toward the pH changes.

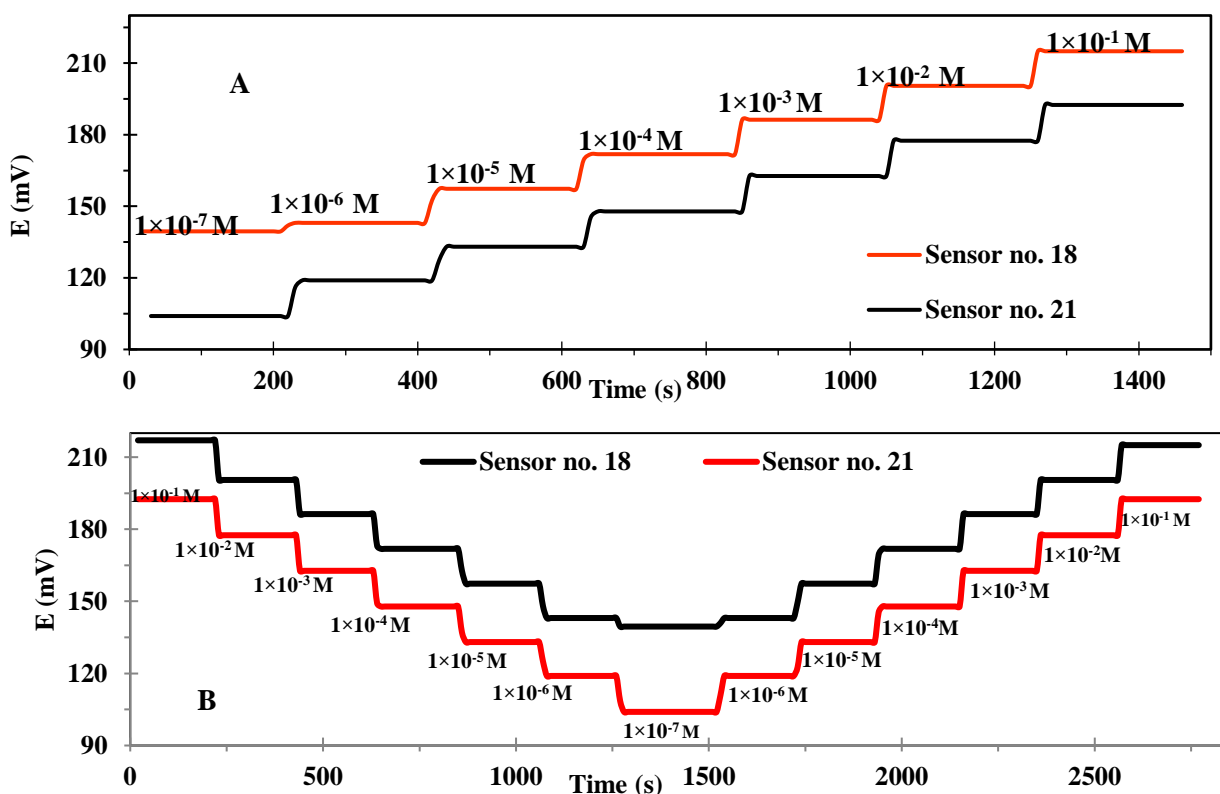


Fig. (3): Dynamic response time (A) and reversibility (B) of sensor no. 18 and sensor no. 21.

According to Fig. 4 the sensors' potential remains stable regardless of the hydrogen ion concentration within the pH range from 3.5 to 6.0 which could be considered the useful pH range. The higher potentials at pHs below 3.5 indicates the sensors' affinity to the hydronium ion ( $\text{H}_3\text{O}^+$ ) as it can fit inside the crown ethers' cavity. Oppositely, the sharp potential decrease at pHs higher than 6.0 results from the formation of insoluble thorium hydroxide complexes and reduction of the free  $\text{Th}^{4+}$  ions in the solution [36].

### 3.4. Selectivity coefficients

The sensors' potentiometric selectivity coefficient values toward various cationic species were calculated and summarized in Table 3. Generally, the selectivity coefficients point out to which extent an interfering ion (j) can affect the sensor's response towards the primary ion, where selectivity coefficient values below 1 indicate the sensor preference for the primary ion [37]. The lower the values of the selectivity coefficient, the less influence the interfering ion will have on the measured potential.

**Table (2): Lifetime of sensor no. 18 and sensor no. 21**

Week	Sensor no. 18		Sensor no. 21	
	Slope, mV decade <sup>-1</sup>	Linear Range, mol L <sup>-1</sup>	Slope, mV decade <sup>-1</sup>	Linear Range, mol L <sup>-1</sup>
1	14.41	$1.0 \times 10^{-6}$ – $1.0 \times 10^{-1}$	14.85	$1.0 \times 10^{-7}$ – $1.0 \times 10^{-1}$
2	14.40	$1.0 \times 10^{-6}$ – $1.0 \times 10^{-1}$	14.86	$1.0 \times 10^{-7}$ – $1.0 \times 10^{-1}$
3	14.53	$1.0 \times 10^{-6}$ – $1.0 \times 10^{-1}$	14.79	$1.0 \times 10^{-7}$ – $1.0 \times 10^{-1}$
4	14.61	$1.0 \times 10^{-6}$ – $1.0 \times 10^{-1}$	14.87	$1.0 \times 10^{-7}$ – $1.0 \times 10^{-1}$
5	14.44	$1.0 \times 10^{-6}$ – $1.0 \times 10^{-1}$	14.78	$1.0 \times 10^{-7}$ – $1.0 \times 10^{-1}$
6	14.52	$1.0 \times 10^{-6}$ – $1.0 \times 10^{-1}$	14.75	$1.0 \times 10^{-7}$ – $1.0 \times 10^{-1}$
8	14.37	$1.0 \times 10^{-6}$ – $1.0 \times 10^{-1}$	14.83	$1.0 \times 10^{-7}$ – $1.0 \times 10^{-1}$
10	14.38	$1.0 \times 10^{-6}$ – $1.0 \times 10^{-1}$	14.79	$1.0 \times 10^{-7}$ – $1.0 \times 10^{-1}$
12	14.31	$1.0 \times 10^{-6}$ – $1.0 \times 10^{-1}$	14.74	$1.0 \times 10^{-7}$ – $1.0 \times 10^{-1}$
14	12.62	$1.0 \times 10^{-5}$ – $1.0 \times 10^{-1}$	13.91	$1.0 \times 10^{-6}$ – $1.0 \times 10^{-1}$
16	11.37	$1.0 \times 10^{-5}$ – $1.0 \times 10^{-1}$	11.74	$1.0 \times 10^{-6}$ – $1.0 \times 10^{-1}$

The selectivity coefficients listed in Table 3 are below 1 which clearly indicates the good selectivity of the developed sensors towards  $\text{Th}^{4+}$  ions in the presence of other ions. The observed behavior can be explained based on the host–guest chemistry; in particular the cavity size of the host molecules which regulates the type of metal cation that can bind within the crown ethers' cavity. The good selectivity of L1 and L2 toward  $\text{Th}^{4+}$  ions is due to the matching of the binding cavity

size of these crowns (1.3–1.6 Å) for the  $\text{Th}^{4+}$  ions (ionic radii 1.05 Å) [38]. The low values of selectivity coefficients for divalent cations highlight their trivial impact on the developed  $\text{Th}^{4+}$  sensors. The non-interfering divalent or trivalent cations are observed to have smaller ionic radii than  $\text{Th}^{4+}$  that result in a loose bonding with the crown ether [39]. Even though  $\text{K}^+$  ion is likely to cause some interference as it has a larger ionic size than  $\text{Th}^{4+}$  ions and can fit to the crown ether cavity.

**Table (3): Selectivity coefficients of sensor no. 18 and sensor no. 21 towards various interfering ions**

Interfering ion (j)	Sensor no. 18	Sensor no. 18
	$\log K_{\text{Th},j}^{\text{pot}}$	$\log K_{\text{Th},j}^{\text{pot}}$
$\text{Li}^+$	-4.25	-4.32
$\text{Na}^+$	-1.24	-1.27
$\text{K}^+$	-0.48	-0.58
$\text{Co}^{2+}$	-3.73	-4.15
$\text{Sr}^{2+}$	-2.59	-3.31
$\text{Ni}^{2+}$	-4.17	-4.42
$\text{Ca}^{2+}$	-2.23	-2.36
$\text{Mg}^{2+}$	-3.11	-3.36
$\text{Mn}^{2+}$	-3.38	-3.90
$\text{Cd}^{2+}$	-3.09	-3.21
$\text{Be}^{2+}$	-4.08	-4.19
$\text{Zn}^{2+}$	-4.42	-4.70
$\text{Cu}^{2+}$	-4.35	-4.52
$\text{Hg}^{2+}$	-3.75	-3.87
$\text{Al}^{3+}$	-4.92	-5.79
$\text{Cr}^{3+}$	-3.52	-3.87

Better selectivity coefficient values were observed for the optimized sensor based on L2 due to the greater rigidity and lipophilicity of L2 compared to L1 which increases the membrane's selectivity. The two tertiary butyl groups in L2 make its structure much more rigid and less flexible compared to L1. This would reduce the approach of other ions and obstructs their complexation in the membrane matrix [39], leading to better selectivity towards  $\text{Th}^{4+}$  ions.

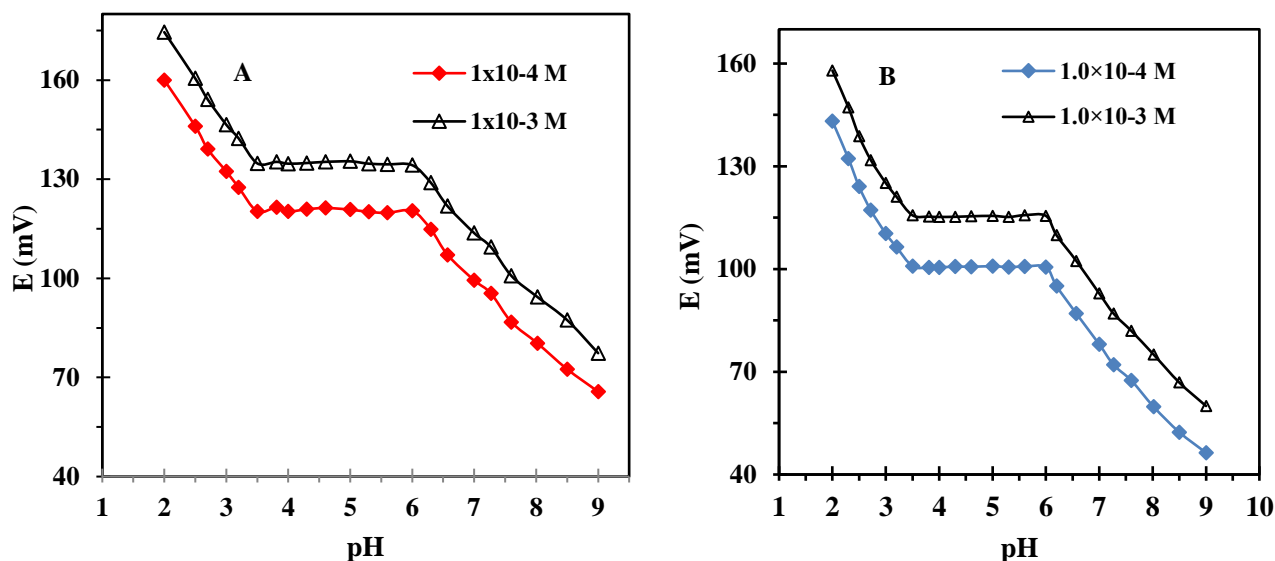


Fig. (4): Effect of pH on the potentials of sensors no. 18 (A) and no. 21 (B) at two  $\text{Th}^{4+}$  ions concentrations.

Table (4): Recovery of  $\text{Th}^{4+}$  ions from different water samples

Sample	Concentration (ppm)*					
	Added	UV	Potentiometry		Recovery (%)	
			Sensor no. 18	Sensor no. 21	Sensor no. 18	Sensor no. 21
Tap water	10	10.15±0.34	9.52±0.51	9.87±0.43	95.20	98.70
	30	30.89±0.10	29.69±0.62	29.75±0.57	98.96	99.16
	50	50.10±0.32	51.34±0.25	49.85±0.15	102.68	99.70
Bottled water	10	9.92±0.35	9.85±0.43	10.06±0.51	98.50	100.60
	30	30.66±0.33	30.02±0.25	29.92±0.25	100.06	99.79
	50	50.89±0.26	51.16±0.85	48.96±0.98	102.32	97.92

\*Average of three measurements ± standard deviation (n=3).

### 3.5. Sensors' repeatability and reproducibility

The sensors' repeatability was examined and expressed in terms of the relative standard deviation (RSD) of the three successive independent intraday measurements of  $\text{Th}^{4+}$  ions over the working concentration ranges of the sensors under similar identical operating conditions. An average Nernstian response of 14.62 and 14.87 mV decade<sup>-1</sup> was obtained with RSD% values of 0.87 and 0.73 for sensors no. 18 and no. 21, respectively indicating the good repeatability of the sensors' response.

The sensor's reproducibility, i.e. the ability to obtain the same result when measuring the same quantity under different conditions, was evaluated using three different optimized membrane sensors prepared at the same time, using identical materials. A similar response with an

average calibration slope values of 14.34 and 14.85 mV decade<sup>-1</sup> and RSD of 1.38 and 1.32 was obtained for sensors no. 18 and no. 21, respectively. The observed variation could result from the thicknesses variation of the different membranes.

### 3.6. Recovery studies

The analytical utility and accuracy of the optimized sensors were evaluated through the recovery studies to determine  $\text{Th}^{4+}$  ions concentration in different water samples following the standard addition procedure. To validate the accurate response of the optimized sensors,  $\text{Th}^{4+}$  ions content was also determined by the reference UV method. The recovery data from potentiometric and UV measurements are presented in Table 4. Based on the obtained data, direct potentiometric measurements have good percentage recovery values that range from 95.20%

to 102.32% and 97.92% to 100.60% for sensors no.18 and no. 21, respectively revealing their high accuracy and precision. The results are close enough to those obtained by the spectrophotometric method, indicating the validity of both sensors to estimate Th<sup>4+</sup> ions concentration effectively.

#### 4. CONCLUSIONS

The development of plasticized PVC membrane sensors incorporating crown ethers as neutral carriers for Th<sup>4+</sup> ions quantification was described in this work. Sensors' optimum performance was attained by a membrane containing 3% crown ether, 1.5% anionic additive (KTpCIPB), 63.5% TEHP as plasticizer, and 32% PVC (w/w%). The optimized sensors showed good potentiometric performance characteristics including high sensitivity, fast response, low detection limit, good repeatability and reproducibility, long-term stability, and selectivity for Th<sup>4+</sup> ions. The optimized sensors were successfully applied in Th<sup>4+</sup> ions determination in various water samples with good accuracy and precision.

#### CONFLICTS OF INTEREST

"There are no conflicts to declare".

#### REFERENCES

- [1] Kang, J.N., Wei, Y.M., Liu, L.C., Han, R., Yu, B.Y., and Wang, J.W., *Appl. Energy*, 2020, vol. 263, no. 1, article. 114602. <https://doi.org/10.1016/j.apenergy.2020.114602>
- [2] Galahoma, A.A., Mohsen, M.Y.M., and Amrani, N., *Nucl. Eng. Technol.*, 2022, vol. 54, no. 1 p.1. <https://doi.org/10.1016/j.net.2021.07.019>
- [3] Humphrey, U.E., and Khandaker, M.U., *Renew. Sust. Energ. Rev.*, 2018, vol. 97, p. 259. <https://doi.org/10.1016/j.rser.2018.08.019>
- [4] Al-Massaedh, A.A., and Khalili, F.I., *J. Radioanal. Nucl. Chem.*, 2021, vol. 327, no.3, p. 1201. <https://doi.org/10.1007/s10967-021-07614-1>
- [5] Nazal, M.K., AlBayyari, M., and Khalili, F.I., *J. Radioanal. Nucl. Chem.*, 2019, vol. 321, no.3, p. 985. <https://doi.org/10.1007/s10967-019-06668-6>
- [6] Zhang, Y., Shao, X., Kong, X., Yin, L., Wang, C., Lin, L., and Ji, Y., *Radiat. Med. Prot.*, 2022, vol. 3, no. 2, p. 91. <https://doi.org/10.1016/j.radmp.2022.03.001>
- [7] Benedik, L., Pilar, A.M., Prosen, H., Jaćimović, R., and Povinec, P.P., *Appl. Radiat. Isot.*, 2021, vol. 175, article 109801. <https://doi.org/10.1016/j.apradiso.2021.109801>
- [8] Jothi, D., Manickam, S., Sawminathan, S., Munusamy, S., Kumar, S., Kumar, S.K.A., and Iyer, S.K., *Dyes Pigm.*, 2022, vol. 197, article 109826. <https://doi.org/10.1016/j.dyepig.2021.109826>
- [9] Masok, F.B., Masiteng, P.L., Mavunda, R.D., Maleka, P.P., and Winkler, H., *J. Radiat. Res. Appl. Sci.*, 2018, vol.11, no. 4, p. 305. <https://doi.org/10.1016/j.jrras.2018.04.003>
- [10] Lindahl, P., Olszewski, G., and Erikss, M., *Appl. Radiat. Isot.*, 2022, vol. 181, article 110103. <https://doi.org/10.1016/j.apradiso.2022.110103>
- [11] Orabi, A.H., Abdou, A.A., Ahmed, S.H., Mahmoud, W.H., and Weheish, H.L., *J. Anal. Chem.*, 2021, vol. 76, no. 3, p. 322. <https://doi.org/10.1134/S1061934821030072>
- [12] Akl, Z.F., and Ali, T.A., *RSC Adv.*, 2016, vol. 6, no. 81, p. 77854. <https://doi.org/10.1039/C6RA14784D>
- [13] Hassanzadeh, P., Yaian, M.R., Baharia, Z., and Matt, D., *J. Chin. Chem. Soc.*, 2013, vol. 53, no. 5, p. 1113. <https://doi.org/10.1002/jccs.200600147>
- [14] Chandra, S., Agarwal, H., and Singh, C.K., *Anal. Sci.*, 2007, vol. 23, no.4, p. 469. <https://doi.org/10.2116/analsci.23.469>
- [15] Khan, A.A., Paquiza, L., and Khan, A., *J. Mater. Sci.*, 2010, vol. 45, no.13, p. 3610. <https://doi.org/10.1007/s10853-010-4407-6>
- [16] Chandra, S., Agarwal, H., Singh, C.K., Sindhu, S.K., and Kumar, P., *Indian J. Chem.*, 2005, vol. 44A, no.10, p. 2060. <https://doi.org/10.2116/analsci.23.469>
- [17] Arida, H.A., Ahmed, M.A., and El-Saied, A.M., *Sensors*, 2003, vol. 3, no. 10, p. 424. <https://doi.org/10.3390/s31000424>
- [18] Ganjali, M.R., Norouzi, P., Faridbod, F., Riahi, S., Yaian, M.R., Zamani, A., and Matt, D., *J. Appl. Electrochem.*, 2007, vol. 37, no.7, p. 827. <https://doi.org/10.1007/s10800-007-9318-0>



- [19] Akl, M.A., and Abd El-Aziz, M.H., *Arab. J. Chem.*, 2016, vol. 9, no. S1, p. S878. <https://doi.org/10.1016/j.arabjc.2011.09.009>
- [20] Chehardoli, G., and Bahmani, A., *Supramol. Chem.*, 2019, vol. 31, no.4, p. 221. <https://doi.org/10.1080/10610278.2019.1568432>
- [21] Golcs, Á., Horváth, V., Huszthy, P., and Tóth, T., *Sensors*, 2018, vol. 18, no. 5, p. 1407. <https://doi.org/10.3390/s18051407>
- [22] Fan, Y., Jia, D., Qin, J., and Huang, Y., *J. Incl. Phenom. Macrocycl. Chem.*, 2020, vol. 98, no. 3-4, p. 205. <https://doi.org/10.1007/s10847-020-01020-y>
- [23] Kim, J., Kim, D.H., Yang, J.C., Kim, J.S., Lee, J.H., and Jung, S.H., *Sensors*, 2020, vol. 20, no. 21, p. 6375. <https://doi.org/10.3390/s20216375>
- [24] Egorov, V.V., Zdrachek, E.A., and Nazarov, V.A., *Anal. Chem.*, 2014, vol. 86, no. 8, p. 3693. <https://doi.org/10.1021/ac500439m>
- [25] Badr, I.H.A., Zidan, W.I., and Akl, Z.F., *Talanta*, 2014, vol. 118, p. 147. <http://dx.doi.org/10.1016/j.talanta.2013.10.011>
- [26] Choi, S., and Yun, J.I., *J. Radioanal. Nucl. Chem.*, 2019, vol. 319, no.1, p. 401. <https://doi.org/10.1007/s10967-018-6342-y>
- [27] Li, L., Yan, Z., and Zhang, S., *J. Iran Chem. Soc.*, 2021, vol. 18, no.11, p. 2853. <https://doi.org/10.1007/s13738-021-02260-6>
- [28] Arvand, M., Zanjanchi, M.A., and Heydari, L., *Sens. Actuators B*, 2007, vol. 122, no. 1, p. 301. <https://doi.org/10.1016/j.snb.2006.05.039>
- [29] Isa, I.Md., Noor, S.M., Juahir, Y., Hashim, N., Ahmad, M., Kamari, A., Mohamed, A., Ghani, S.A., and Wardani, N.I., *Int. J. Electrochem. Sci.*, 2014, vol. 9, no.8, p. 4512.
- [30] Zdrachek, E., and Bakker, E., *Anal. Chem.*, 2021, vol. 93, no.1, p. 72. <https://doi.org/10.1021/acs.analchem.0c04249>
- [31] Pietrzak, K., Wardak, C., and Cristóvão, B., *Ionics*, 2022, vol. 28, no. 5, p. 2423. <https://doi.org/10.1007/s11581-022-04482-x>
- [32] Ahmed, Y.M., Badawy, S.S., and Abdel-Haleem, F.M., *Microchem. J.*, 2022, vol. 177, article 107276. <https://doi.org/10.1016/j.microc.2022.107276>
- [33] Hadisaputra, S., Canaval L.R., Pranowo, H.D., and Armunanto, R., *Monatsh. Chem.*, 2014, vol. 145, no. 5, p.737. <https://doi.org/10.1007/s00706-013-1129-x>
- [34] Buck, R.P., and Lindner, E., *Pure Appl. Chem.*, 1994, vol. 66, no. 12, p. 2527. <http://dx.doi.org/10.1351/pac199466122527>
- [35] Kopylovich, M.N., Mahmudov, K.T., and Pombeiro, A.J.L., *J. Hazard. Mater.*, 2011, vol. 186, no. 2-3, p.1154. <https://doi.org/10.1016/j.jhazmat.2010.11.119>
- [36] Kumar, R.S., Kumar, S.K.A., Vijayakrishna, K., Sivaramakrishna, A., Rao, C.V.S.B., Sivaraman, N., and Sahoo, S.K., *Anal. Methods*, 2019, vol. 11, no.10, p. 1338. <https://doi.org/10.1039/C8AY02740D>
- [37] Chandra, S., Sharma, K., and kumar, A., *J. Saudi Chem. Soc.*, 2014, vol. 18, no.4, p.555. <https://doi.org/10.1016/j.jscs.2011.11.002>
- [38] Rounaghi, G.H., Mohajeri, M., Tarahomi, S., and Rahmanian, R., *J. Solution Chem.*, 2011, vol. 40, no.3, p. 377. <https://doi.org/10.1007/s10953-011-9651-0>
- [39] Han, W.S., Lee, Y.H., Jung, K.J., Ly, S.Y., Hong, T.K., and Kim, M.H., *J. Anal. Chem.*, 2008, vol. 63, no.10, p. 987. <https://doi.org/10.1134/S1061934808100110>